OPEN ACCESS

Spectral behavior of the linear polarization degree at right-angle scattering configuration for nanoparticle systems

New Journal of Physics
The open-access journal for physics

Spectral behavior of the linear polarization degree at right-angle scattering configuration for nanoparticle systems

B Setién, P Albella, J M Saiz, F González and F Moreno[1]
Grupo de Óptica, Departamento de Física Aplicada, Universidad de Cantabria, Avda de los Castros S/N, 39005 Santander, Spain
E-mail: morenof@unican.es

New Journal of Physics **12** (2010) 103031 (14pp)
Received 10 May 2010
Published 19 October 2010
Online at http://www.njp.org/
doi:10.1088/1367-2630/12/10/103031

Abstract. We present a numerical study of the spectral evolution of the linear polarization degree at right-angle scattering configuration ($P_L(90^\circ)$) for two different particle systems: an isolated nanosphere and a nanodimer composed of two finite size spherical particles separated by a gap distance d. We shall focus on the influence of charge oscillation modes other than the dipolar on the linear polarization degree of the scattered light. The possibility of using this alternative parameter for characterizing nanoparticle systems and particle interaction is analyzed.

Contents

[1] Author to whom any correspondence should be addressed.

1. Introduction

The term 'nanoparticle' (NP) is used for particles of size within the range 1–100 nm. The use of NPs has grown at the same rate as their applications in nanotechnology. NPs have been shown to be a basic element of many applications, such as markers and sensors in biomedicine, molecular spectroscopy enhanced by surfaces, surface enhanced Raman scattering (SERS), the manufacture of new opto-electronic devices, etc [1]–[4]. An important example in medicine is the use of plasmonic resonances for evaluating the success of NPs in chemotherapy cancer treatment by analyzing the patterns of light scattered by the cellular structures involved [5]. The shape and size of the NPs are key to finding suitable applications [6, 7]. For these reasons, the characterization of such particles has become an important issue. A typical way to assess geometrical parameters is by using microscopy (electronic, confocal, etc). However, it is well established that light scattering techniques provide excellent methods for determining the optical and geometrical parameters of those particles. Furthermore, scattering techniques show interesting advantages: they are non-invasive and can provide results in real time. Metallic NPs have become the focus of attention of many researchers in photonic areas because of their capability to exhibit local surface plasmon resonances (LSPRs) [8]. LSPRs occur when a metal NP is illuminated by electromagnetic radiation (usually, visible) whose wavelength (frequency) is able to produce a resonant collective oscillation of the free electrons of the metal with maximum amplitude. In general, the spectral shape and position of those resonances depend on the size, shape and optical properties of NPs and also on the surrounding environment [7]. Then, the measurement of scattering and extinction spectral cross sections and, in particular, the shape and position of the resonant peaks constitutes a well-established method for determining the optical and morphological properties of metallic NPs. Apart from the spectral behavior of the scattered intensity, there are other parameters of the electromagnetic radiation such as its polarization [9] that, in many cases, as we will see in the following, represent an alternative method for determining not only particle parameters but also the electromagnetic configuration of the particle (electric charge oscillation modes) when it is excited with selected values of the incident frequency out of the dipolar resonance. In particular, in this work we will focus on analysis of the spectral behavior of the linear degree of polarization of the scattered radiation, measured at 90° to the direction of propagation of the exciting radiation, $P_{\mathrm{L}}(90^{\circ})$, defined as the ratio between $(I_{\perp} - I_{\parallel})$ and $(I_{\perp} + I_{\parallel})$, with $I_{\perp}$ and $I_{\parallel}$ being the scattered intensities at 90° with polarizations perpendicular and parallel to the scattering plane, respectively.

Plasmon resonances in metallic isolated spherical NPs can be studied with the Mie theory [10]. For particles very small compared to the wavelength, the spectral behavior is dominated by the dipolar oscillation as corresponds to the quasi-static approximation. Under the Mie theory view, this is interpreted as if the scattered electromagnetic field were dominated by the first term in its series expansion and the spectrum of the extinction cross section presents a resonant peak for a frequency for which the real part of the dielectric constant is approximately -2. In this case, $P_{\mathrm{L}}(90^{\circ}) = 1$ ($I_{\perp}$ is isotropic in the plane of incidence, while $I_{\parallel}$ is eight-shaped with its null at 90° with respect to the incident direction). As the particle size increases, more terms have to be included in that series because other modes higher than the dipolar one start to oscillate. For instance, quadrupolar electric resonances manifest when the real part of the dielectric constant is close to -1.5. This generates scattered fields with $P_{\mathrm{L}}(90^{\circ}) \neq 1$. Quadrupolar resonances are not as sensitive to the particle size as the dipolar ones

but they contain information about the particle when its size is in a range where the dipolar resonances are weaker and very broad, say, when the particle size is in the range 50–100 nm.

The use of NPs as nanotechnological tools has also found interesting applications when they are used as a group, forming aggregates. Let us cite as an example the case of the simplest aggregate, the metallic nanodimer, i.e. a set of two linked spherical NPs. In this case, the plasmonic spectrum is affected not only by the morphological properties of its constituents (shape and size) but also by the interaction between the nanospheres [11]. This interaction obviously depends on the interparticle separation, an important parameter in establishing the local fields associated with a dimer [12]–[14]. The high values of the electric and magnetic fields at the junction region are due to coupling between electromagnetic (EM) fields of each nanosphere that is widespread and depends on the gap distance between them; the closer the particles, the greater the interaction [15]. This configuration is now being used for optical nanosensors by controlling the nanodimer size. For gold nanodimers, it has been shown that these can detect small proteins and small organic molecules [16]. Also, analyses of the plasmonic resonances that appear for these dimers in terms of separation between their components have shown that they are useful for measuring distances at the nanoscale for biological systems. These are known in the literature as 'nanorulers' [17].

As outlined previously, most of the research performed either on isolated metallic NPs or on their aggregates is based on analyzing the intensity of light scattered by these systems as the wavelength of the incident radiation changes. In particular, this analysis is based on the spectral evolution of the resonant peaks that appear in the spectrum of either the extinction or the scattering cross sections: changes in the plasmonic spectrum, whiskers [18], landslides and the appearance of new peaks (higher-order modes). In this work, we propose an analysis of the polarization of scattered light, as an alternative technique to the analysis of the spectral evolution of the multipole resonances for characterizing scattering systems composed of metallic NPs. In particular, we will study the spectral evolution of the degree of linear polarization of the scattered light, P_{L}, at 90° scattering angle. This will be done for the two most representative cases, that of the isolated particle and that of the particle dimer. In the case of an isolated spherical particle the appearance of new resonant modes above the dipolar one is linked with an increment in size; then, $P_{\mathrm{L}}(90^{\circ})$ serves as a tool for obtaining information on the size of the NPs in the system. Moreover, in the case of the dimer, $P_{\mathrm{L}}(90^{\circ})$ is a useful tool to identify the interaction between the resonant modes of the constituent NPs, as well as its orientation and position.

This paper is structured as follows: section 2 introduces the basic theory, section 3 describes both the scattering configurations and the geometries analyzed in this research, section 4 presents the main results and, finally, section 5 summarizes the most important conclusions.

2. Theoretical basis

In order to understand the meaning of the parameter $P_{\mathrm{L}}(90^{\circ})$, it is useful to revisit the Mie theory [10]. For a non-magnetic ($\mu = 1$) spherical particle of radius R, illuminated by a monochromatic plane wave, the scattered field can be expressed as a multipolar expansion of vector spherical harmonics (VSH) as

$$\boldsymbol{E}_{\mathrm{s}} = \sum_{n=1}^{\infty} E_n (\mathrm{i} a_n \boldsymbol{N}^{(3)}_{\mathrm{e\,ln}} + b_n \boldsymbol{M}^{(3)}_{\mathrm{o\,ln}}), \tag{1}$$

where $E_n = \mathrm{i}^n E_0(2n+1)/(n(n+1))$, and a_n and b_n are the diffusion coefficients of the Mie theory that depend on the optical properties, size and shape of the particle. The two components of the scattered intensity with polarizations parallel, $I_\parallel$, and perpendicular, $I_\perp$, to the scattering plane are proportional to the squared diagonal elements of the scattering matrix [10] and they are given by

$$\begin{aligned} I_\parallel &\propto \left| \sum_{n=1}^{\infty} \frac{(2n+1)}{n(n+1)} (a_n \pi_n + b_n \tau_n) \right|^2, \\ I_\perp &\propto \left| \sum_{n=1}^{\infty} \frac{(2n+1)}{n(n+1)} (a_n \tau_n + b_n \pi_n) \right|^2, \end{aligned} \tag{2}$$

where τ_n and π_n are well-defined angular functions of the scattering angle θ, measured with respect to the incident direction. In the scattering plane, the linear polarization degree of the scattered light, $P_\mathrm{L}(\theta)$, is defined as

$$P_\mathrm{L}(\theta) = \frac{I_\perp(\theta) - I_\parallel(\theta)}{I_\perp(\theta) + I_\parallel(\theta)}. \tag{3}$$

For a nanosphere very small compared to the wavelength of the incident beam ($R \ll \lambda$), the expression of the EM scattered field is dominated by the first terms of the series expansion given by equation (2). In this case, the two most important scattering coefficients are a_1 and b_1, which correspond to the EM dipole modes of the electric charge oscillation. These coefficients are given by the following expressions:

$$\begin{aligned} a_1 &= -\frac{\mathrm{i}2x^3}{3} \frac{\varepsilon - 1}{\varepsilon + 2} + O(x^5), \\ b_1 &\approx O(x^5), \\ a_n &= b_n = O(x^5); \quad \forall n \geqslant 2, \end{aligned} \tag{4}$$

where a non-magnetic particle ($\mu = 1$) has been assumed, ε being its dielectric constant and $x = 2\pi R/\lambda$ its size parameter. When the approximation given by equation (4) holds, the scattering particle behaves, electromagnetically speaking, as a dipole. In this case, the degree of linear polarization at $\theta = 90^\circ$ is equal to unity. By increasing the size of the particle, the amount of light scattered increases and also higher-order modes start to contribute to the scattered EM wave. Let us assume that the dipolar ($n = 1$) and quadrupolar ($n = 2$) terms constitute a good approach to the EM behavior of the particle. If we substitute from equations (2) and (4) for the first two terms, $n = 1, 2$, we obtain an approximation of the linear polarization degree P_L for unpolarized incident light, which for $\theta = 90^\circ$ takes the following form:

$$P_\mathrm{L}(90^\circ) = \frac{(9a_1 - 15b_2)^2 - (9b_1 - 15a_2)^2}{(9a_1 - 15b_2)^2 + (9b_1 - 15a_2)^2}. \tag{5}$$

What makes this parameter very interesting is that, for NPs, it is equal to 1 unless some non-dipolar behavior takes place. This is the case for a resonant quadrupolar oscillation produced either by an increase of size or by some particle–particle interaction. In figure 1, we show polar diagrams for the parallel (a) and perpendicular (b) intensities scattered by a silver [19]

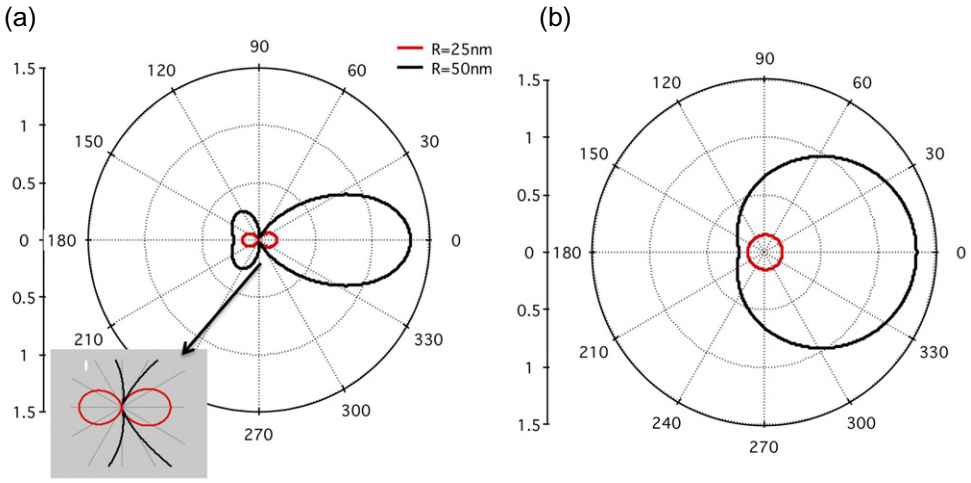

Figure 1. Polar diagrams of the scattered intensity with components (a) parallel ($I_{\parallel}$) and (b) perpendicular ($I_{\perp}$) to the scattering plane for a silver NP at $\lambda \approx 350\,\text{nm}$ (0° and 180° correspond, respectively, to forward and backward scattering).

NP for two values of the particle radius, $R = 25$ and $R = 50\,\text{nm}$. The incident wavelength has been chosen as $\lambda = 350\,\text{nm}$. As can be seen, by increasing the NP size, the amount of light scattered increases. Moreover, the scattered intensity with parallel polarization ($I_{\parallel}$) loses the typical '8-shape' of the scattered electric field of the radiated wave by a dipole and does not get a value close to zero around 90° any more (at 90°, $I_{\perp}/I_{\parallel} \approx 100$ for $R = 25\,\text{nm}$ and $I_{\perp}/I_{\parallel} \approx 6$ for $R = 50\,\text{nm}$ (see the inset in figure 1(a)). Also, $I_{\perp}$ tends to lose the usual circular symmetry shown by a radiating dipole source. In both cases, these trends are a consequence of the influence of the modes with order n equal to or higher than 2 (equation (2)).

Following this line of reasoning, figure 2 shows an analysis of the theoretical model presented above. For a single metallic sphere made of silver with $R = 50\,\text{nm}$, figure 2(a) shows the spectral evolution of the total scattered intensity calculated at right scattering angle, $I_{\text{sca}}(90°) = (I_{\perp} + I_{\parallel})$ (continuous red line), and also the contributions of the parallel (continuous black line) and perpendicular (dotted blue line) components. This size has not been selected in an arbitrary way, since we need a particle big enough to present charge oscillating modes higher than the dipolar one. For comparison, in the inset, the spectrum corresponding to a smaller particle, $R = 25\,\text{nm}$, is also shown. As can be seen in figure 1, for this particle size, dipole scattering behavior is clearly observed. In this case, the scattered intensity measured at 90° is dominated by the perpendicular component because the parallel one is negligible at this scattering angle. We can also appreciate the dipolar behavior of this small particle because of the presence of a single sharp resonance around $\lambda \approx 360\,\text{nm}$.

If we now focus on the bigger particle, the structure of $I_{\text{sca}}(90°)$ as a function of λ clearly changes. Apart from a resonant peak at $\lambda \approx 386\,\text{nm}$ corresponding to the dipolar charge oscillation mode, the presence of a shoulder around $\lambda \approx 352\,\text{nm}$ is clearly seen. The latter comes from the quadrupolar charge oscillation mode due to the bigger size of the particle and consequently to the increment in degrees of freedom for the oscillation of the conduction band electrons in the silver particle. By looking at the parallel intensity curve (continuous black line in

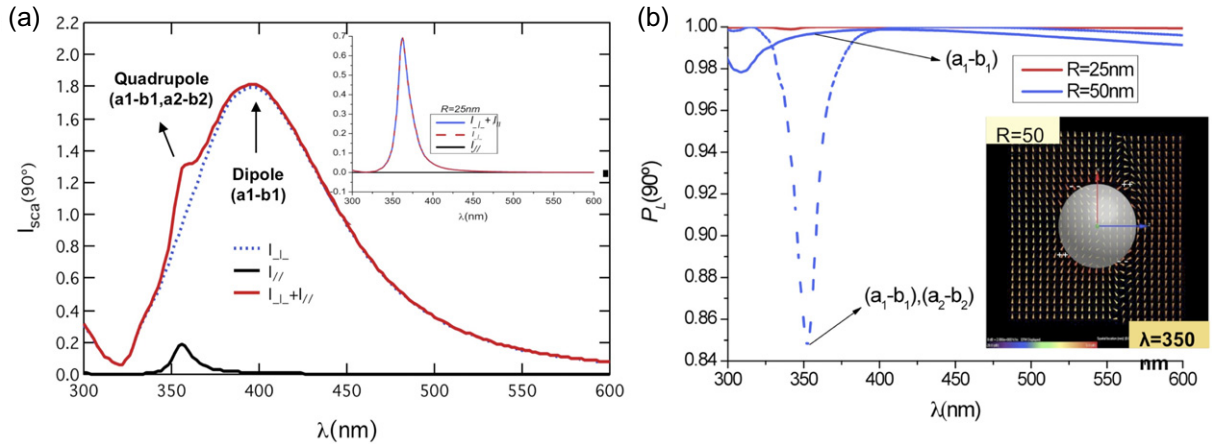

Figure 2. (a) Scattered intensities: parallel ($I_{\parallel}$) and perpendicular ($I_{\perp}$) to the scattering plane and $I_{\rm sca} = (I_{\perp} + I_{\parallel})$ calculated at $\theta = 90^{\circ}$ for a silver spherical nanoparticle of $R = 50\,$nm. The inset corresponds to $R = 25\,$nm. (b) Linear polarization degree, $P_{\rm L}(90^{\circ})$, for a silver spherical particle (red, $R = 25\,$nm, and blue, $R = 50\,$nm) as a function of the incident wavelength. The inset shows the distribution of the local electric field in and around the NP of $R = 50\,$nm. Inside the particle this clearly corresponds to a quadrupolar charge distribution. The incident beam is a plane wave ($\lambda = 350\,$nm) linearly polarized parallel to the X-axis (in red) and propagating in the $-Z$-direction (the Z-direction corresponds to the blue axis).

figure 2(a)), we can easily assign each peak to each resonance effect. In the first case, the peak in parallel intensity at about 352 nm is due to the quadrupolar radiation and gives the shoulder seen in the total scattered intensity. If this were not present, there should be no parallel-polarization radiation at 90° as in the case of the particle with $R = 25\,$nm. This is the case for the peak around 386 nm, where $I_{\parallel} = 0$. This indicates that this corresponds to a resonance with dipolar character. Furthermore, it has suffered a red-shift, as compared to the spectral position of the dipolar peak of the smaller particle. In figure 2(a) we have also included an indication of the most important Mie terms of equation (1) that contribute to the charge oscillation modes whose corresponding radiated electromagnetic fields give the total scattered intensity. For instance, the maximum contribution to the dipolar peak comes from the a_1 and b_1 terms, while for the quadrupolar mode (the shoulder) we have to include the a_2 and b_2 terms in order to describe this behavior. In figure 2(b), a similar study to that shown in figure 2(a) is carried out, but this time by means of the polarimetric parameter, $P_{\rm L}(90^{\circ})$, defined in equations (3) and (5). This study has provided us with useful information for identifying each resonance. When only the dipolar mode is excited for a given incident wavelength, the parallel intensity radiated at 90° is negligible; therefore the value of $P_{\rm L}$ is very close to 1. However, when the quadrupolar mode is excited at about 352 nm, $I_{\parallel}$ is not zero any more and, consequently, the value of $P_{\rm L}$ deviates from 1, reaching a minimum at the exact quadrupolar excitation wavelength. As an illustration of this effect, we show in the inset of figure 2(b) the calculated electric field distribution, by using a numerical method based on FDTD, in both the proximities and inside the silver spherical particle of radius 50 nm when this is illuminated in the $-Z$-direction (from the right side of the figure) by a plane wave of $\lambda = 350\,$nm.

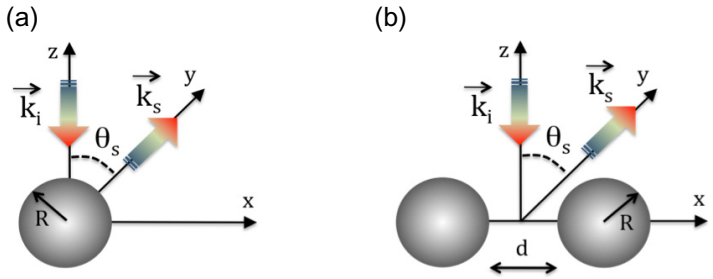

Figure 3. Description of scattering geometries for (a) a single sphere and (b) a metallic dimer. The scattering plane is located in the *ZY*-plane.

In general, metallic NPs with $R < 30$ nm scatter light as if they were little radiating dipoles; the parallel intensity, $I_{\parallel}$, is equal to 0 at $\theta = 90^{\circ}$ and therefore $P_{\mathrm{L}} = 1$. In this case, the contribution from the quadrupolar EM terms (a_2, b_2) is negligible compared to that from the homologous dipole terms (a_1, b_1). This situation can be observed in figures 2(a) and (b) in the curves corresponding to $R = 25$ nm. In this case, the radiating characteristics of the particle are those of a dipole and the result does not depend on the coefficents a_2 and b_2. However, for particles larger than approximately 30 nm, the coefficients a_1 and b_1 are not enough for describing the scattering characteristics of the system. We only find the dipolar resonance, but the quadrupolar excitation around $\lambda \approx 350$ nm is not observed unless the coefficient a_2 is introduced. In this way, $P_{\mathrm{L}}(90^{\circ})$ becomes an indicator of the type of charge oscillation that is being induced in the particle.

This theory was developed for calculating the scattering of symmetric assemblies of single spherical particles. For particles with diameters smaller than 100 nm, only the first two terms of that expansion (dipolar terms) make a significant contribution. As particle size increases, more terms must be considered. These higher-order terms can excite new resonances that perturb the typical '8-shaped' spatial distribution obtained for the light-scattering pattern of a dipole when it is illuminated with a p-polarized wave (parallel to the scattering plane). As shown by our results, the influence of the presence of multipolar modes can be found through an analysis of the polarimetric properties of the scattered light.

To conclude this section, we want to point out that, in general, numerical methods based on the Mie theory are a robust way of analyzing scattering systems composed of isolated particles. However, for solving more complex scattering systems composed of several particles, going from dimers to systems formed by multiple particles, there is a range of numerical methods available and designed to deal with more general systems. In this work, we have used the *T*-matrix method [20, 21]. The results will be shown in the following sections.

3. System description

To better understand the usefulness of measuring the parameter $P_{\mathrm{L}}(90^{\circ})$, we will first consider the case of a spherical silver particle with radius ranging from 20 to 100 nm (see figure 3(a)). Then, we will consider a dimer, composed of two spherical silver particles each with size similar to the aforementioned case and separated by a gap of distance d (see figure 3(b)). In this second case, we have analyzed two different geometries: (i) the symmetric dimer (SD), formed by two identical particles, and the asymmetric dimer (AD) with particles of different size, R_1

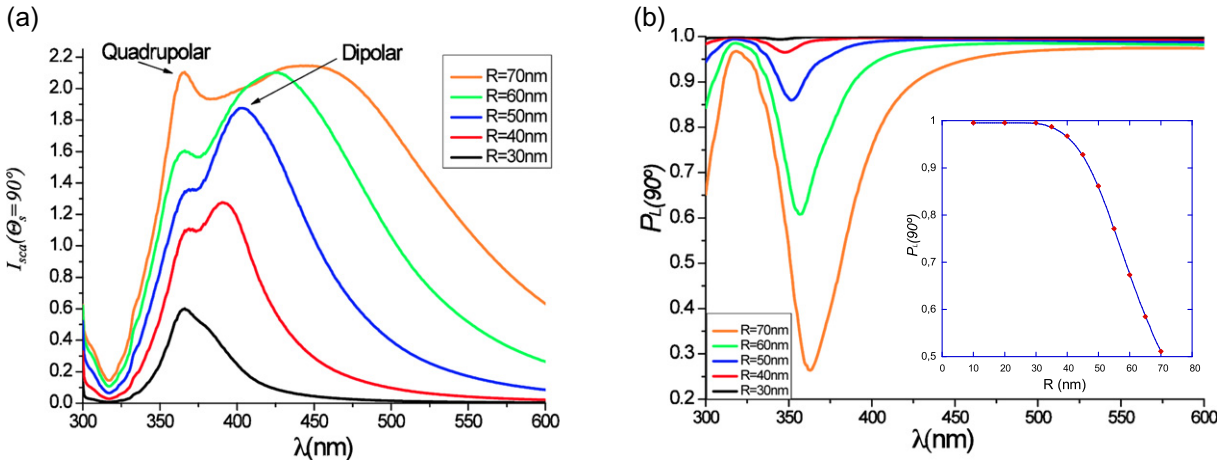

Figure 4. (a) Scattered intensity, $I_{\mathrm{sca}}(90^\circ)$, and (b) linear polarization degree, $P_{\mathrm{L}}(90^\circ)$, of a spherical silver particle as a function of the incident wavelength for several sizes. The inset in (b) shows the evolution of the values of the minimum of the linear polarization degree, $P_{\mathrm{L}}(90^\circ)$, as a function of particle size.

and R_2. Also note that, although all cases in the previously specified particle size range have been studied, only the most representative ones are plotted in the forthcoming figures. These cases are sufficient to show the evolution of the curves in the analyzed range with clear plots.

In all cases, the plane YZ is the scattering plane and the incident beam always travels in the $-Z$-direction (figures 3(a) and (b)). It is a depolarized beam, i.e. all possible orientations of the electric field in the transversal plane XY are equally possible. Scattered light is observed along the Y-axis, i.e. right-angle scattering intensities corresponding to the field parallel or perpendicular to the scattering plane. $I_{\parallel}$ and $I_{\perp}$ are calculated in order to determine $P_{\mathrm{L}}(90^\circ)$. For the dimer case, we have chosen the configuration with the two particles aligned along the X-axis and illuminated along the Z-direction. This is because in this situation, particle interaction is stronger, there is no shadowing effect and the retardation effects do not exist in either the illumination or the scattered light.

4. Results

4.1. Isolated particle

The case of the isolated silver NP is shown in figure 4(a), where $I_{\mathrm{sca}}(90^\circ)$ is plotted for spheres of sizes ranging from $R = 30\,\mathrm{nm}$ to $R = 70\,\mathrm{nm}$. For small particles, $R < 30\,\mathrm{nm}$, the dipolar behavior is dominant, therefore exhibiting a single resonance peak. This resonance broadens and red-shifts as the particle size increases. At the same time (and as expected) a new peak, due to the quadrupolar resonance, appears at lower wavelengths. This peak does not shift significantly with an increase of particle size, and the corresponding resonance can be easily assessed by means of the linear polarization degree calculated at right scattering angle. This parameter is plotted in figure 4(b) where it reaches a minimum where the quadrupolar resonance is excited. This minimum shifts to the red, although very slightly, as the particle size increases. More drastic is the change in depth of the minimum. This increases with particle size, starting to

be significant for NPs with $R > 30$ nm. The inset in figure 4(b) shows the evolution of the values of the minimum of $P_L(90^\circ)$ with particle size. This result suggests that the measurement of P_L at a convenient wavelength may constitute a tool for NP size determination in the range of 50–100 nm.

4.2. Metallic dimer

Once we have proved that $P_L(90^\circ)$ can be useful for identifying the presence of resonant modes of higher order than the dipolar, and consequently, that it is potentially useful for determining the size of NPs, we will move to a more complex system, consisting of two spherical silver NPs (silver nanodimer). This is the simplest scattering system where multiscattering effects and their influence on the parameter P_L can be analyzed. In this case, excited resonances are not only those corresponding to each particle forming the aggregate but also those related to the interaction between the NPs. The spectral structure of the resonances will depend not only on the size of the NPs forming the dimer, but also on the separation distance between them.

We first analyze the case of a dimer consisting of two identical silver spheres (SD) located along the X-axis and with $d = 3$ nm (see figure 3(b)). In figure 5 we show, as an example, the right-angle scattered intensity and $P_L(90^\circ)$ spectra (observed in the Y-axis direction) for sizes ranging from $R = 20$ nm to $R = 50$ nm. For small particles the system shows one main resonance located around $\lambda = 415$ nm (see figure 5(a)). This resonance is red-shifted from the original resonance position of the isolated particle of $R = 20$ nm. This is due to the interaction between the nanospheres, and this shift increases with the size of the particle.

For $R = 20$ nm, a small peak centered at $\lambda = 352$ nm is observed. This peak is typically quadrupolar and is observed for the isolated particle only in the case of big NPs (see the inset of figure 5(a) for an example). Then, a system with two particles, even though very small (20 nm), exhibits a plasmonic right-angle spectrum similar to that of a single particle of larger effective size. Obviously, when the size of the NPs forming the dimer increases, these effects are seen more clearly. Figure 5(b) shows the spectral linear polarization degree, $P_L(90^\circ)$, calculated for the same group of SDs ($R = 20$–50 nm and $d = 3$ nm). The parameter $P_L(90^\circ)$ presents a minimum (about $\lambda = 350$ nm) whose magnitude increases with the constituent particle radius. This minimum corresponds to the wavelength where the plasmonic quadrupolar resonance appears for isolated NPs (fingerprint of the NP), although with a deeper fall from 1.

Apart from the quadrupolar fingerprint in P_L, a second minimum can be observed that slightly shifts to the red as the size of the dimer constituents increases. The spectral position of this minimum is strongly correlated with that of the minimum in $I_{sca}(\theta_s = 90)$. It is important to emphasize here that $I_\perp$ dominates the scattered intensity. For our scattering configuration, at $\theta = 90^\circ$, the existence of the second minimum in P_L is due to the decrease of $I_\perp$ in this spectral zone, where $I_\parallel$ ($\ll I_\perp$) is monotonic. Obviously, this second minimum in P_L is a clear indication of the interaction of the dimer particles. It appears because the dipolar plasmon red-shifts as the size of the particles increases, while the quadrupolar mode associated with the isolated particle remains in the same spectral location. In other words, the dipolar contribution is weakened (inhibited by particle interaction) in the spectral range where $I_\perp$ is minimum. It is also interesting to remark that the extinction efficiency, Q_{ext}, follows a similar spectral behavior as $I_{sca}(\theta_s = 90)$ when the incident beam is linearly polarized with its electric vector parallel to the line connecting the particle centers (s-polarized in our notation) [22]. A minimum of I_{sca} in a given spectral region corresponds to a minimum of Q_{ext}. In other words, the second minimum of

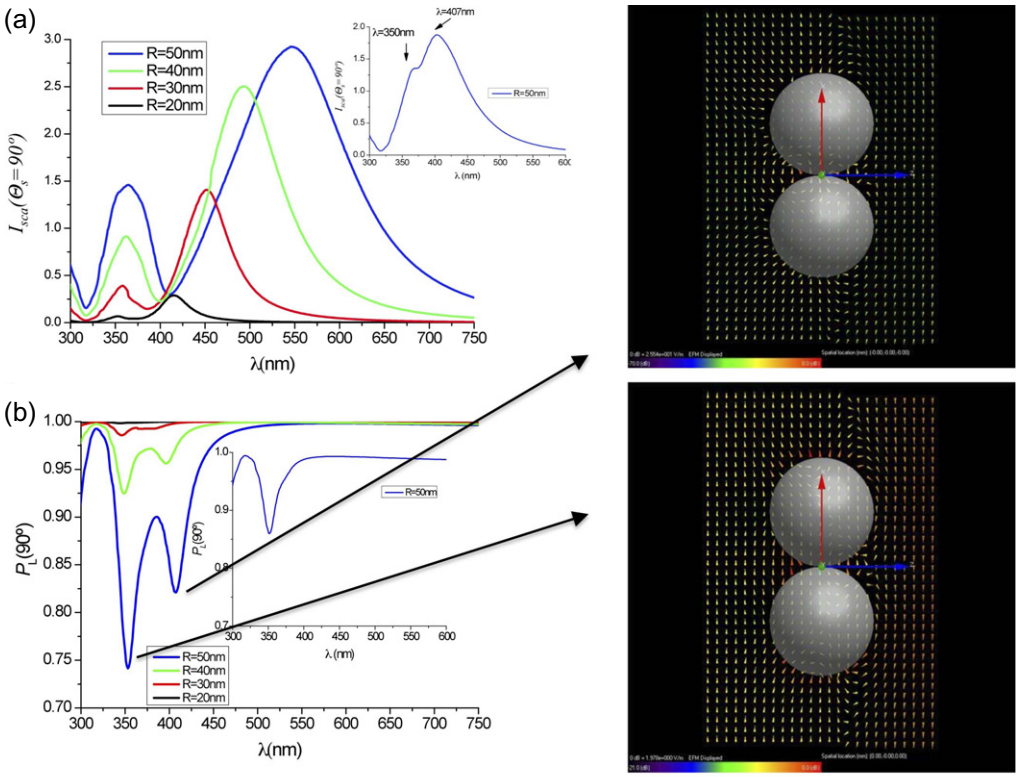

Figure 5. (a) Right-angle scattered intensity, $I_{\mathrm{sca}}(90^\circ)$, and (b) right-angle linear polarization degree, $P_{\mathrm{L}}(90^\circ)$, produced by a silver dimer of spherical particles as a function of the incident wavelength for several values of the particle radius. Inset of (a): spectrum of $I_{\mathrm{sca}}(90^\circ)$ for an isolated silver NP of $R = 50\,\mathrm{nm}$. Inset of (b): $P_{\mathrm{L}}(90^\circ)$ for the isolated particle case. The two right figures show the near electric field distributions for $R = 50\,\mathrm{nm}$ corresponding to the first and second minima of P_{L} in (b), as indicated by the black arrows. The incident beam is a plane wave linearly polarized parallel to the X-axis (in red) and propagating in the $-Z$-direction (the Z-direction corresponds to the blue axis).

P_{L} indicates that for a given short distance between particles, and within a given spectral range, incident light is less extinguished due to particle interaction. This curious property shown by silver NPs also means that NP interaction can increase transmission at the proper frequencies but also that it can be monitored through the measurement of P_{L} at right scattering angles. This parameter summarizes particle size effects and also the inhibition of the dipolar contribution due to particle interaction.

To go further in this interpretation, we study the spectral behavior of $I_{\mathrm{sca}}(90^\circ)$ and $P_{\mathrm{L}}(90^\circ)$, for a dimer composed of two silver NPs of different size (AD, see figure 6). We choose particle sizes in such a way that one of them has a sufficient size ($R = 50\,\mathrm{nm}$) so as to produce two resonances, dipolar and quadrupolar (see the inset of figure 5(a)), whereas the other is chosen small enough so as to exhibit only the dipolar plasmon resonance ($R = 20\,\mathrm{nm}$). Both $I_{\mathrm{sca}}(90^\circ)$ and $P_{\mathrm{L}}(90^\circ)$ are studied as a function of the particle distance, ranging from $d = 0\,\mathrm{nm}$ (in contact) to $d = 10\,\mathrm{nm}$ (see figure 6). For $d = 10\,\mathrm{nm}$, interaction is very weak and the constituent particles can be considered independent. $I_{\mathrm{sca}}(90^\circ)$ behaves similarly to the isolated NP case

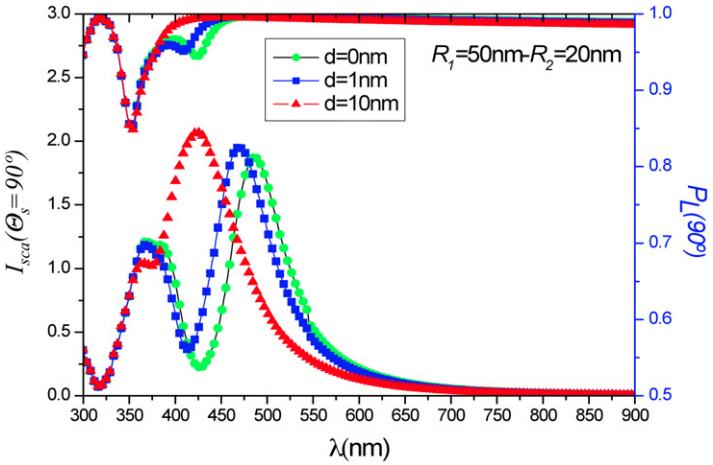

Figure 6. Light scattered intensity ($I_{\mathrm{sca}}(90^\circ)$) and linear polarization degree $P_{\mathrm{L}}(90^\circ)$ at $\theta = 90^\circ$ for an AD of Ag as a function of the incident wavelength, with varying gap distance, d.

(a quadrupolar resonance at $\lambda = 360$ nm and a dipolar one around $\lambda = 425$ nm). This result indicates that the system behaves as if we illuminated a single effective particle slightly bigger than 50 nm (both maxima, $\lambda = 360$ nm and $\lambda = 425$ nm, match with the peaks for $R = 60$ nm. When the two NPs are very close ($d = 1$ nm or in contact), $I_{\mathrm{sca}}(90^\circ)$ shows a dipolar plasmon resonance at even longer wavelengths with respect to the previous case, and also another plasmon resonance at $\lambda = 360$ nm. This corresponds to the position where the quadrupolar resonance appears for the isolated particle. Again, the system behaves as an 'effective NP' of radius slightly larger than 50 nm.

If we now analyze the spectral behavior of $P_{\mathrm{L}}(90^\circ)$, we see that when the NPs are separated by a distance longer than 10 nm, $P_{\mathrm{L}}(90^\circ)$ shows a single minimum around $\lambda = 354$ nm, corresponding to the position of the quadrupolar plasmon resonance of the system. In these conditions, the coupling between both particles, large and small, is negligible. When the particles are close enough, a new minimum appears for wavelengths between 400 and 450 nm, but its depth is smaller than that shown for the symmetric case. This is a clear indication that the parameter P_{L} gives information not only about particle interaction but also about its strength. Again, this second minimum evolves in the same way as that of $I_{\mathrm{sca}}(90^\circ)$. The result, as a whole, is consistent with the discussion of $P_{\mathrm{L}}(90^\circ)$ in the case of an SD. Consequently, $P_{\mathrm{L}}(90^\circ)$ appears as an interesting parameter to identify or monitor dimer formation for given size pairs.

Finally, we have studied the spectral behavior of $I_{\mathrm{sca}}(90^\circ)$and $P_{\mathrm{L}}(90^\circ)$ in the case of illuminating an SD containing two silver NPs of radius $R = 50$ nm and different values of d. The spectral behavior of $P_{\mathrm{L}}(90^\circ)$ and $I_{\mathrm{sca}}(90^\circ)$ is shown in figure 7. Concerning the intensity, the maximum corresponding to the dipolar resonance shifts to larger wavelengths as d decreases, producing the effect of higher effective particle size. The peak corresponding to the quadrupolar resonance remains in approximately the same position and with the same size as in the isolated particle case.

If we analyze the behavior of $P_{\mathrm{L}}(90^\circ)$, we observe that for $d = 10$ nm, the structure, although wider, is quite similar to that found for isolated particles. The left minimum appears in the same place ($\lambda \approx 350$ nm, position corresponding to the quadrupolar resonance), but

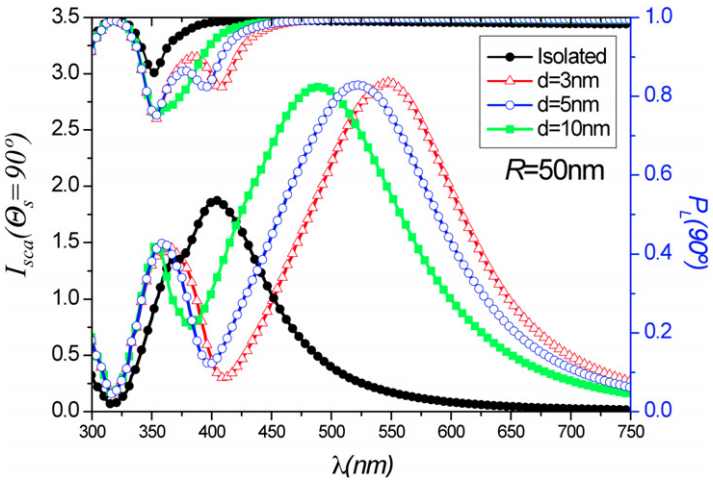

Figure 7. Light scattered intensity, $I_s(90^\circ)$, and linear polarization degree, $P_L(90^\circ)$, at $\theta = 90^\circ$ for an SD of Ag of $R = 50$ nm as a function of the incident wavelength, and for different values of the gap distance, d.

with a significantly higher departure from 1, because the interaction enhances the quadrupolar resonance. By decreasing the distance d, a second minimum appears at longer wavelengths. Again, the position of this new minimum shifts to longer wavelengths as the two particles meet, the same as $I_{sca}(90^\circ)$. This proves again the sensitivity of $P_L(90^\circ)$ to the coupling of electrical fields generated by the charge distributions in the particles.

Although in this work we have used silver as the basic material, similar conclusions can be reached for gold. As gold does not show resonances as sharp as those for silver in the wavelength range analysed, the spectral behavior of $P_L(90^\circ)$ for gold does not show such a nice sharp peak at the position of the quadrupolar resonances and also where the interacting effects are larger (see figures 5 and 6). Instead, P_L presents a more global deviation from unity where multipolar effects appear, evolving in a similar way as silver, when the particle size changes or multiple scattering exists.

5. Conclusions

The spectrum of the scattered intensity produced by either metallic NPs or arbitrary nanostructures contains features (spectral position and width of peaks, intensity values and slopes, shifts, etc) for the analysis of which new characterizing techniques in the nanometric range have been developed. As the scattered electromagnetic radiation can be determined not only by its intensity but also by its polarization, this parameter provides us with additional information, which if conveniently exploited can provide us with new characterizing alternatives in the world of nanotechnology.

In this work, we have shown one of these alternative techniques based on the right-angle measurement of the spectrum of the linear polarization degree, P_L, calculated from the radiation scattered by metallic NPs either isolated or interacting with other particles. It has been seen that the analysis of the spectral response of this parameter can bring new complementary ways for characterizing nanostructures. In fact, for the isolated particle case, the spectral analysis of P_L

shows its sensitivity to the presence of scattering modes other than the dipolar. This feature is closely related to particle size and also, in a more general case, to particle anisotropy. This suggests that the measurement of P_L as a function of the incident wavelength can generate potential methods for NP sizing. Also, for the case of NP aggregates, we have seen how the value of P_L provides us with additional information complementing that obtained with the intensity spectrum. P_L provides more detailed information about the interaction of particles. At present, we are trying to generalize the application of the method proposed in this work to more complex nanostructures (for instance, nanoshells) and also to particles with magnetic properties for their interest in biomedical applications.

Acknowledgments

We acknowledge financial support from USAITCA (US Army International Technology Center—Atlantic) under the project R&D1390-PH-01 and from the Ministry of Education of Spain under the project FIS2007-60158. The authors gratefully acknowledge the support and also the computer resources provided by the Red Española de Supercomputación node Altamira at the Instituto de Fisica de Cantabria. BS thanks USAITCA for support through a grant. We thank Dr Gorden Videen for his useful comments.

References

[1] Aslan K, Lakowicz J R and Geddes C D 2004 Nanogold plasmon resonance based glucose sensing *Anal. Biochem.* **330** 145–55
[2] Wang T and Lin W 2006 Electro-optically modulated localized surface plasmon resonance biosensors with gold nanoparticles *Appl. Phys. Lett.* **89** 173903
[3] Li W, Camargo P H C, Lu X and Xia Y 2009 Dimers of silver nanospheres: facile synthesis and their use as hot spots for surface-enhanced Raman scattering *Nano Lett.* **9** 485–90
[4] Large N, Abb M, Aizpurúa J and Muskens O 2010 Photoconductively loaded plasmonic nanoantenna as building block for ultracompact optical switches *Nano Lett.* **10** 1741–6
[5] Lal S, Clare S E and Halas N J 2008 Nanoshell-enabled photothermal cancer therapy: impending clinical impact *Acc. Chem. Res.* **41** 1842–51
[6] Aslan K, Lakowicz J R and Geddes C D 2005 Plasmon light scattering in biology and medicine: new sensing approaches visions and perspectives *Curr. Opin. Chem. Biol.* **9** 538–44
[7] Kelly K L, Coronado E, Zhao L L and Schatz G 2003 The optical properties of metal nanoparticles: the influence of size, shape and dielectric environment *J. Phys. Chem.* B **107** 668–77
[8] Prasad P N 2004 *Nanophotonics* (New York: Wiley-Interscience)
[9] Bohren C F 1990 Sizing nanoparticles by means of elliptically polarized scattered light: a suggested method *Part. Part. Syst. Charact.* **7** 107–12
[10] Bohren C F and Huffman D R 1983 *Absorption and Scattering of Light by Small Particles* (New York: Wiley)
[11] García de Abajo F J 2008 Nonlocal effects in the plasmons of strongly interacting nanoparticles, dimers and waveguides *J. Phys. Chem.* **112** C 17983–7
[12] Xu H, Aizpurúa J, Käll M and Apell P 2000 Electromagnetic contributions to single-molecule sensitivity in surface-enhanced Raman scattering *Phys. Rev.* E **62** 4318–24
[13] Bouhelier A, Beverluis M R and Novotny L 2003 Characterization of nanoplasmonic structures by locally excited photoluminescence *Appl. Phys. Lett.* **83** 5041–3
[14] Zelenina A S, Quidant R and Nieto-Vesperinas M 2007 Enhanced optical forces between coupled resonant metal nanoparticles *Opt. Lett.* **32** 1156–8

[15] Romero I, Aizpurúa J, Bryant G W and García de Abajo F J 2006 Plasmons in nearly touching metallic nanoparticles: singular response in the limit of touching dimers *Opt. Express* **14** 9988
[16] Acimovic S, Kreuzer M P, Gonzalez M U and Quidant R 2009 Plasmon near-field coupling in metal dimers as a step toward single molecule sensing *ACS Nano* **3** 1231–7
[17] Reinhard B J, Siu M, Agarwal H, Alivisatos A P and Liphardt J 2005 Calibration of dynamic molecular rulers based on plasmon coupling between gold nanoparticles *Nano Lett.* **5** 2246–52
[18] Hillenbrand R and Aizpurúa J 2009 Light sources: coloured heat *Nat. Photonics* **5** 609–10
[19] Palik E D 1985 *Handbook of Optical Constants of Solid* (New York: Academic)
[20] Mackowski D W and Mishchenko M I 1996 Calculation of the T matrix and the scattering matrix for ensembles of spheres *J. Opt. Soc. Am.* A **13** 2266–78
[21] Mackowski D W 1991 Analysis of radiative scattering for multiple sphere configurations *Proc. R. Soc.* **433** 599–614
[22] Chen R-L, Liu X-X and Chang C-C 2007 Particle plasmons of metal nanospheres: application of multiple scattering approach *Phys. Rev.* E **76** 016609